Implementation of the Tanimura-Mimura's Strain Rate Dependent Constitutive Model in LS-DYNA® Using User Defined Material Model

Dr. T. Tsuda[1], Dr. S. Tanimura[2],
Dr. A. Abe[3], Dr. M. Katayama[3], Dr. T. Sakakibara[3]
[1] *ITOCHU Techno-Solutions Corporation, Miyahara, Yodogawa-ku, Osaka, Japan*
[2]*Aichi University of Technology, Gamagori, Aichi, Japan*
[3]*ITOCHU Techno-Solutions Corporation, Kasumigaseki, Chiyoda-ku, Tokyo, Japan*

Abstract

Tanimura-Mimura constitutive model covers a wide range of the strain rates and of a large strain, and enables us to use unified and common material constants to simulate the dynamic behaviors of materials and/or bodies. In this paper, dynamic behaviors of high speed tensile tests, buckling tests and crash test of a full vehicle are simulated by implementing this model in LS-DYNA®. Obtained numerical results are in good agreement with the experimental ones and the validity of the model has been demonstrated.

Introduction

In order to consider the strain rate effect on dynamic behavior of materials in a numerical analysis code, the Cowper-Symonds model, the Johnson-Cook model and the Zerilli-Armstrong model, etc. are used typically. However, in these constitutive models, it is necessary to choose the values of the required parameters by performing dynamic tests and/or by referring to sundry records for each material concerned in advance. A lot of time and the effort are also required to do so.

Tanimura and Mimura newly developed a practical constitutive model [1][2][3][4]. Based on the systematic results of the dynamic tensile properties obtained by using the Sensing Block Type High Speed Material Testing System (SBTS) for ferrous metals, aluminum alloys and copper alloys, Tanimura, et al. obtained a set of values of parameters of the model specified for each material group of ferrous metals, aluminum alloys and copper alloys. They also showed that the new constitutive model and the unified set of values of parameters of this model are useful to simulate the dynamic stress-strain curves of any material belonging to the material group of ferrous metals, aluminum alloys or copper alloys.

This model has two remarkable features. The first is that this model (T-M model) can be applied more easily not only to the homogenous deformation region, but also to a wide range of deformation reaching the true fracture strain, over a wide strain rate range (10^{-2} s^{-1} ~ 10^{4} s^{-1}). The second is that the obtained set of parameters for the model can be used to any material belonging to the material group of ferrous metals, aluminum alloys or copper alloys, as long as only the quasi-static stress-strain curve of the material concerned is known in advance.

We implemented this Tanimura-Mimura model in LS-DYNA® using the user defined material model in cooperation with Tanimura. In this paper, we show that the model is applicable to a wide variety of dynamic behaviors and it is very convenient to use and effective.

Tanimura-Mimura's strain rate dependence constitutive model

Tanimura-Mimura's strain rate dependence constitutive model is shown in Eq. (1).

$$\sigma = \sigma_s + \left[\alpha \cdot (\varepsilon^p)^{m1} + \beta\right] \cdot \left(1 - \frac{\sigma_s}{\sigma_{CR}}\right) \cdot \ln\left(\frac{\dot{\varepsilon}^p}{\dot{\varepsilon}_s^p}\right) + B(\varepsilon^p) \cdot \left(\frac{\dot{\varepsilon}^p}{\dot{\varepsilon}_u}\right)^{m2} \qquad (1)$$

where σ is the flow stress, σ_s is the stress at a lower plastic strain rate $\dot{\varepsilon}_s^p$, ε^p is the plastic strain, $\dot{\varepsilon}^p$ is the plastic strain rate, $\dot{\varepsilon}_s^p$ is the lower limit value of strain rate range and chosen as 10^{-2} s^{-1} for the tested material group, $\dot{\varepsilon}_u$ is the unit of strain rate (=1 s^{-1}), σ_{CR} is the critical stress under uniaxial tension or compression, $\alpha, \beta, m1, m2$ are material parameters specified for each material group, and B is the coefficient of the viscous term of the flow stress specified for each material group. The first term in the right side of Eq. (1) represents the quasi-static stress, the second the incremental flow stress depends on the strain rate, and the third the dramatic increase of stress at a high strain rate range (we call this term a viscous term in this paper).

User Defined Material Model in LS-DYNA®

The T-M model has been implemented in LS-DYNA using the user defined material model. The main input parameters in *MAT_USER_DEFINED_MATERIAL_MODELS are the material type number and the quasi-static stress-strain curve of the material concerned, in addition to the material density and the Young's modulus and the Poisson's ratio, etc. The material parameters ($\alpha, \beta, m1, m2, \sigma_{CR}$ and B) specified for each material group were obtained by Tanimura, et al. and were embedded in subroutine UMAT42. Therefore, it is necessary to input the identification number of the unit of mass, length and time. The input deck for this material is defined as follows:

```
*MAT_USER_DEFINED_MATERIAL_MODELS
$ Units: mm, sec, ton, N
$      mid        ro        mt       lmc       nhv    iortho     ibulk        ig
         1 2.700E-09        42        16         4                  4         5
$    ivect     ifail    itherm    ihyper      ieos

$     MTYP         E        NU         K         G      ETAN      SIGY        NP
         2  6.90e+04      0.33 6.765E+04 2.594e+04                          -2
$   NUNITM    NUNITL    NUNITT
         4         1         3
*DEFINE_CURVE
$     lcid      sidr       sfa       sfo      offa      offo    dattyp
         2
$                a1                  o1
             0.000            269.0000
          0.0100000            293.5000
             :                   :
          3.8000000           1040.8000
```

We have implemented this T-M constitutive model in LS-DYNA which can be applied to solid element and shell element for three material groups, that is the ferrous metals, aluminum

alloys which exhibit the positive strain rate sensitivity, and some of aluminum alloys which exhibit the negative sensitivity or almost non sensitivity.

Verification analyses

(1) High Speed Tensile Test

A series of tensile tests using the tensile test pieces shown in Fig. 1 (b) for a wide range of strain rates were performed by Tanimura, et al. using the Sensing Block Type High Speed Material Testing System (SBTS, Saginomiya, INC.) [3],[4],[5].

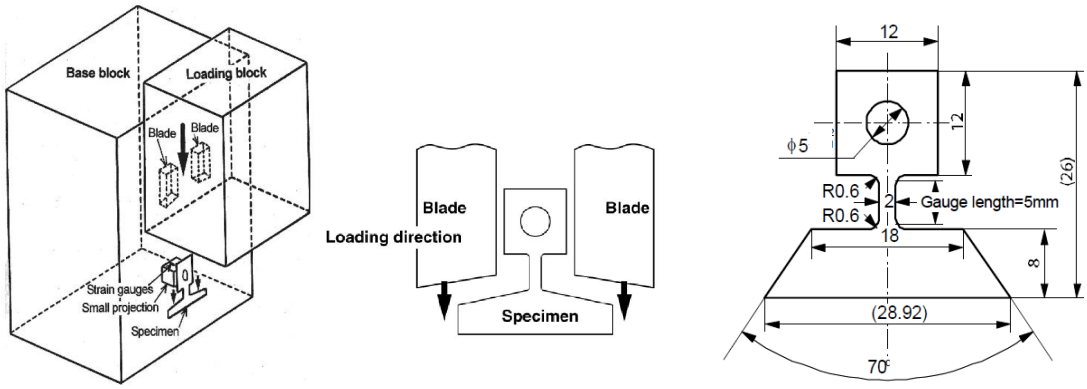

(a) Tensile testing device (b) Test piece geometry

Fig. 1 Testing device of the sensing block method

Figure 2 (a) shows a verification analysis model which is the gauge length part of the test piece shown in Fig. 1 (b), and the size is 5 mm in length, 2 mm in width and 1 mm in thickness for SPCC metal and 2 mm in thickness for A 6061-T6. Numerical simulations were carried out with LS-DYNA using the T-M model. A FE mesh of the verification analysis model is shown in Fig. 2 (b). The element type in LS-DYNA employed in the simulation is constant stress solid element and the mesh size is 0.05 mm. The constant loading velocity (5 m/s) corresponding to the strain rate of 10^3 s^{-1} was applied to the model side with the fixed boundary condition on another side.

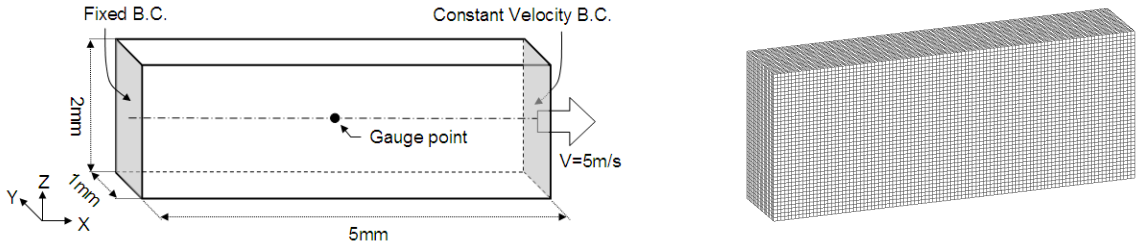

(a) Simulation model geometry (b) Finite element mesh

Fig. 2 Simulation model

SPCC belonging to BCC metal and A6061P-T6 belonging to FCC metal were employed as the verification materials, because the dynamic property of material strength of these materials is

greatly different. The material constants and the quasi-static (strain rate 10^{-2} s^{-1}) stress-strain curves required as input data for this T-M constitutive model are shown in Table 1 and Fig. 3.

Table 1 Material Constants of SPCC and A6061P-T6

		SPCC	A6061-T6
Mass density	(ton/mm^3)	7.86E-9	2.70E-9
Young's modulus	(MPa)	2.10E+5	6.90E+4
Poisson's ratio	(-)	0.28	0.33

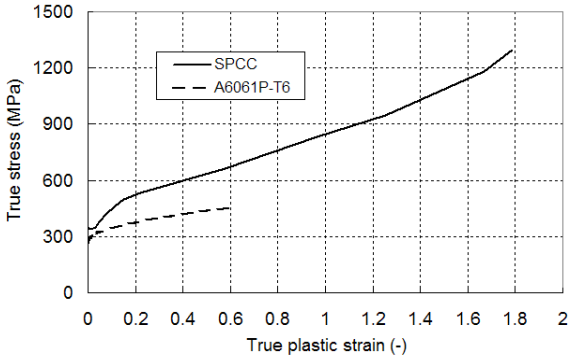

Fig. 3 Stress-strain curves at quasi-static condition of SPCC and A6061P-T6

The stress-strain curves obtained by the experiment and the simulation for SPCC and A6061P-T6 are shown in Fig. 4. The thick-gray curve and the thick-light-gray curve indicate the measurement results in the homogenous deformation region (for strain from 0 % to 20 %) before starting the necking at strain rate 10^3 s^{-1} and 10^{-2} s^{-1}, respectively. The circular symbols indicate the measurement points obtained by measuring the cross section size of the necking part at each time for the incremental deformation whose original strain rates, corresponding to the homogenous deformation, is 10^{-2} s^{-1}[3][4]. The broken curve indicates the simulation result using the T-M model at the gauge point shown in Fig. 2 (a). The dotted curve indicates the simulation result with no strain rate effect at the gauge point shown in Fig. 2 (a) and is same to the quasi-static stress-strain curve (10^{-2} s^{-1}) shown in Fig. 3. The solid curve shown in Fig. 4 (a) indicates the stress-strain curve of the T-M model at strain rate 10^3 s^{-1} obtained by substituting directly the quasi-static stress-strain curve of SPCC and the set of material parameters of ferrous metals group into the Eq. (1). We call here this solid curve an ideal solution curve. We can observe that, in Fig. 4 (a), the experimental results (thick-gray curve), the ideal solution of T-M model (solid curve) and the simulation result with T-M model (broken curve) are match well. It is thus clear that Tanimura-Mimura constitutive model represent the strain rate effect with high accuracy, in a wide range of strain from the homogenous deformation region to the large strain reaching the fracture strain.

Relational curves between the equivalent plastic strain rate and the equivalent plastic strain obtained by the simulation at the gauge point shown in Fig. 2 (a) are shown in Fig. 5. We can observe that the simulation curve (broken curve) shown in Fig. 4 becomes slightly higher than the ideal solution curve (solid curve), which may be caused by the occurrence of the higher strain rates than 10^3 s^{-1} after the occurrence of the necking as shown in Fig. 5. Furthermore, even though the strain rates in the necking part are increased with increasing strain as shown in Fig. 5 (a), the simulation curve (broken curve), the ideal solution curve of T-M model (solid curve) and the quasi-static curve (dotted curve) converge as the strain increases as shown in Fig. 4 (a).

These phenomena may be understood by considering that the dependency of the strain rates on the flow stress becomes rapidly low as the strain increases especially for the ferrous materials.

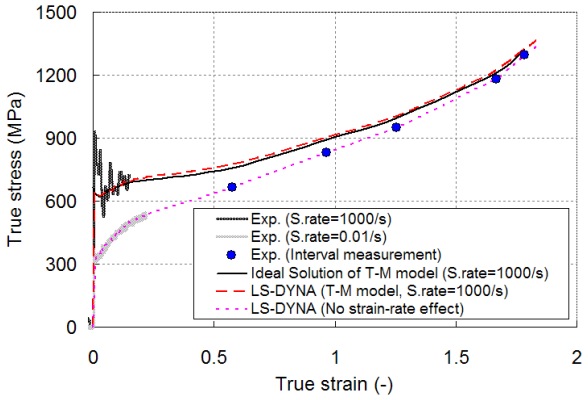

(a) SPCC

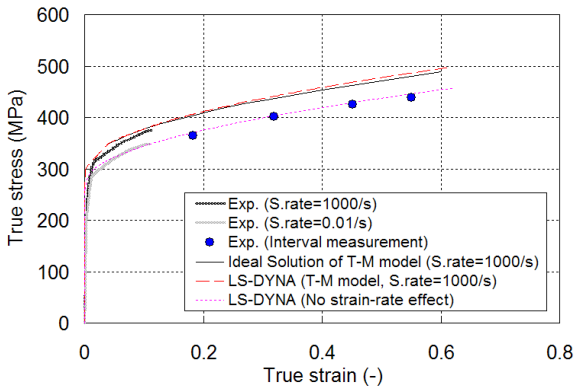

(b) A6061P-T6

Fig. 4 Stress-strain curves

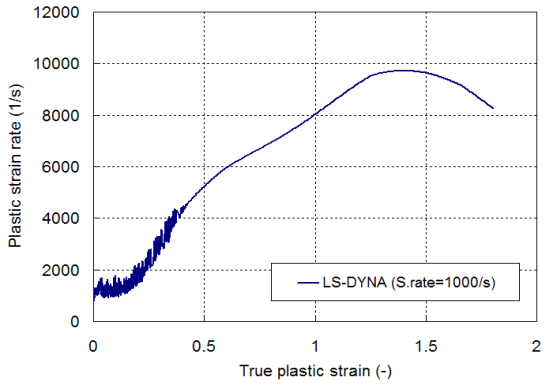

(a) SPCC

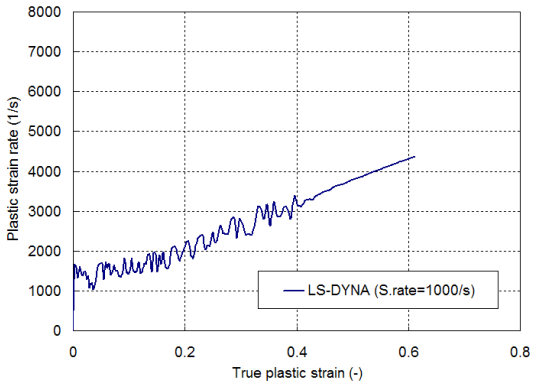

(b) A6061P-T6

Fig. 5 Plastic strain rate curve

The necking shape and the cross section shape at the fracture (fracture strain: 180 % [3]) of the experiment and the simulation for SPCC are shown in Fig. 6 and Fig. 7 respectively. The necking shape and the cross section shape at the fracture (fracture strain:61 % [4]) of the experiment and the simulation for A6061P-T6 are, likewise, shown in Fig. 8 and Fig. 9 respectively. Although the fracture position of the simulation result is sifted from the experimental result for SPCC, necking shape and cross section shape of the simulated results by LS-DYNA with the T-M model are coincident with the experimental results fairly well for both materials.

Specimen geometries of the gauge length portion and the cross sectional areas at the fracture occurrence are summarized comparing with the simulation results in Table 2. Lengths of the gauge length portion after fracture of the experiment and the simulation for SPCC are 7.188 mm and 7.06 mm respectively, and the error is 1.8 %. The cross sectional area at the fracture of the experiment and the simulation result for SPCC are 0.351 mm^2 and 0.331 mm^2 respectively, and the error is 5.7 %. The error for the case of A6061P-T6 is 2.3 %.

We can thus conclude that the T-M model is useful to simulate the dynamic deformation behaviors in high accuracy not only in the homogenous deformation region but also in the large deformation region reaching the fracture strain and it is very effective.

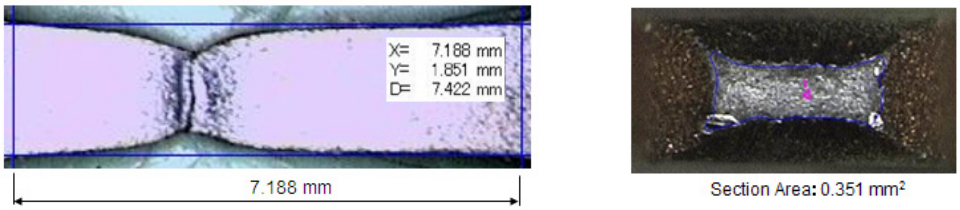

(a) Necking shape (b) Cross section shape

Fig. 6 Experimental results of SPCC

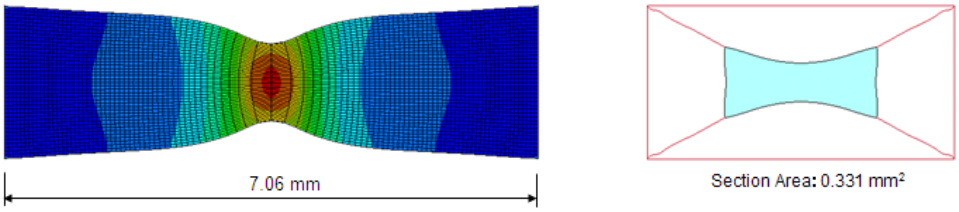

(a) Necking shape (b) Cross section shape

Fig. 7 Simulation results (LS-DYNA applied T-M model) of SPCC

(a) Necking shape (b) Cross section shape

Fig. 8 Experimental results of A6061P-T6

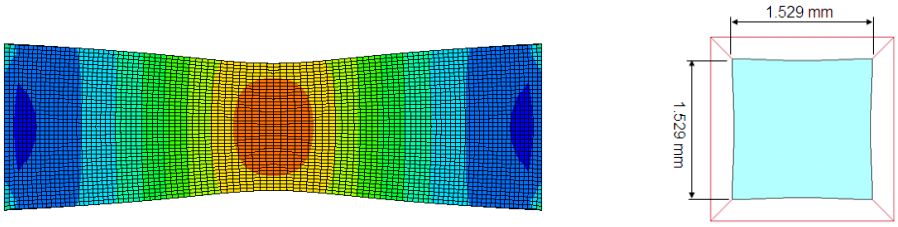

(a) Necking shape (b) Cross section shape

Fig. 9 Simulation results (LS-DYNA applied T-M model) of A6061P-T6

Table 2 Comparison of specimen size after fracture

		Experiment	LS-DYNA	Error
SPCC model	Gauge length (mm)	7.188	7.06	1.8 (%)
	Cross sectional area (mm^2)	0.351	0.331	5.7 (%)
A6061P-T6 model	Cross sectional area (mm^2)	2.393	2.338	2.3 (%)

(2) Impact Buckling Test

The Sensing Block Type Dynamic Buckling Testing System (SBDBTS) developed by Tanimura, et al. [5] is shown in Fig. 10 (a). The dynamic buckling tests for circular tubes and simulations as shown in Fig. 10 (b) were performed to verify the Tanimura-Mimura constitutive model. A drop-weight of 90 kg in mass was freely dropped from 2.66 m (Case-1) and 2.72 m (Case-2) in height on the top of the tube as shown in Fig. 10 (b), and the impact force applied onto the top of the tube and the displacement of the top face of the tube were measured. The specimen size is 45 mm in diameter, 100 mm in length and 2 mm in thickness. Numerical simulations were carried out about 1/4 area of the specimen with symmetric conditions and the FE mesh of the verification simulation model is shown in Fig. 10 (c). The specimen's model was divided into 4 elements along thickness direction, 200 elements along longitudinal direction and 18 elements along hoop direction respectively with constant stress solid element. The drop-weight and the floor were modeled using rigid body. The friction coefficient between the floor and the specimen was 0.15.

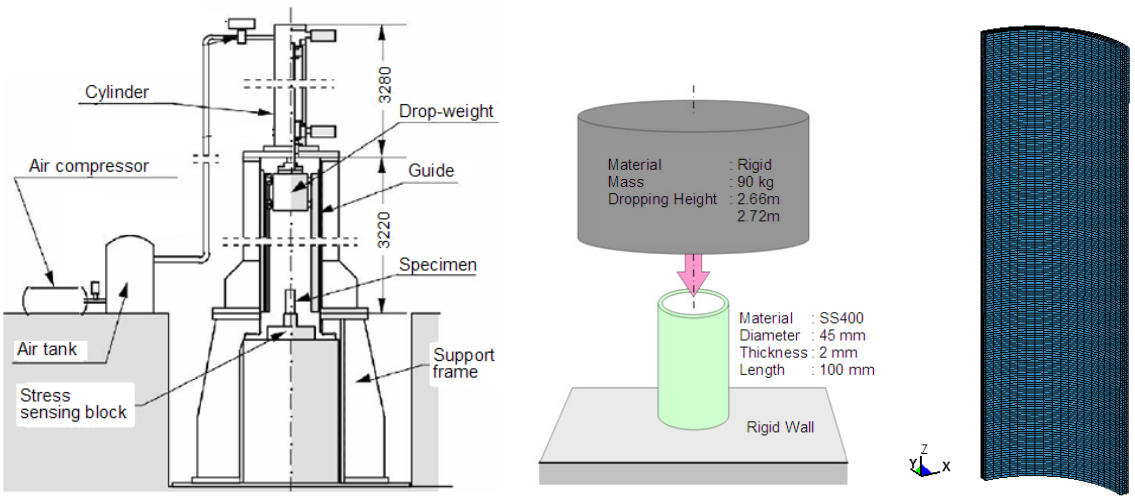

(a) Test equipment (b) Specimen size (c) FEM mesh

Fig. 10 Dynamic buckling test of circular tube

The material employed as the verification material in the dynamic buckling test is SS400. The material constants and the quasi-static (strain rate 10^{-2} s^{-1}) stress-strain curves requested as input data in this T-M constitutive model are shown in Table 3 and Fig. 11 respectively.

Table 3 Material Constants of SS400

		SS400
Mass density	(ton/mm^3)	7.85E-9
Young's modulus	(MPa)	2.09E+5
Poisson's ratio	(-)	0.28

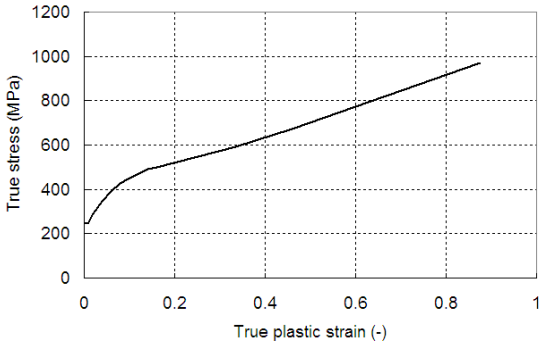

Fig. 11 Stress-strain curves at quasi-static condition of SS400

Deformation geometries of the tube after the impact of Case-1 (dropping height: 2.66 m) and Case-2 (dropping height: 2.72 m) are shown in Fig. 12 and Fig. 13 respectively. Experimental results, simulation results with the T-M model and simulation results with no strain rate effect are shown in Fig. 12 (a), (b) and (c), respectively. The deformation geometries of the simulation results are 1/2 model generated by making mirror copies of 1/4 model of the specimen. It was observed that local buckling was occurred at the bottom of tube, and the numbers of the buckling rumples observed in the experiment and the simulation with the T-M model were both one and a half, and the number of it in the simulation with no strain rate effect was two.

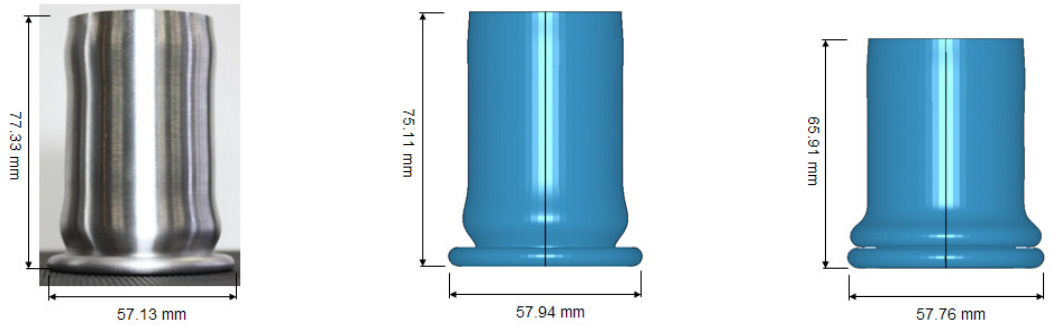

(a) Experiment (b) LS-DYNA(T-M model) (c) LS-DYNA(No strain rate effect)

Fig. 12 Final shape of SS400 specimen after impact (Case-1)

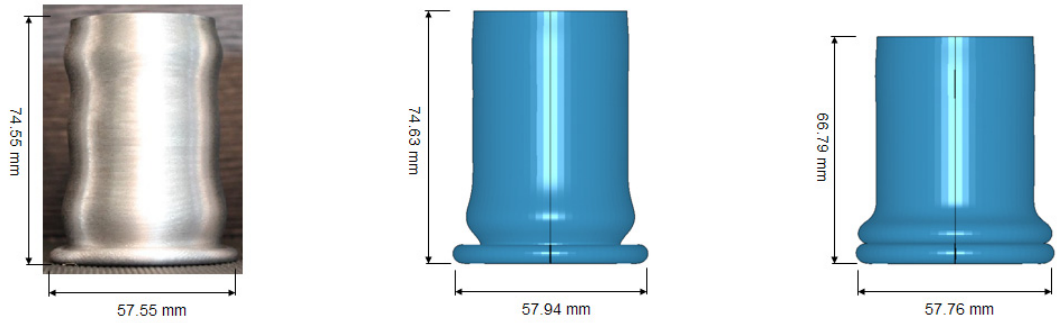

(a) Experiment (b) LS-DYNA(T-M model) (c) LS-DYNA(No strain rate effect)

Fig. 13 Final shape of SS400 specimen after impact (Case-2)

The measurement values of the height and the diameter of the tubes after the buckling were shown in Table 4. We can see that the differences between the results of the simulation with the T-M model and of the experiment are within 3%.

Table 4 Comparison of specimen size after buckling

		Experiment	LS-DYNA	Error
Case-1 (Dropping height=2.66m)	Length (mm)	77.33	75.11	2.9 (%)
	Outer diameter (mm)	57.13	57.94	1.4 (%)
Case-2 (Dropping height=2.72m)	Length (mm)	74.55	74.63	0.1 (%)
	Outer diameter (mm)	57.55	57.94	0.7 (%)

The impact force caused by the drop-weight to the displacement of the upper face of the tube of Case-2 (dropping height: 2.72 m) are shown in Fig. 14. The solid curve indicates the experimental results, the broken curve indicates the simulation results with the T-M model and the dotted curve indicates the simulation results with no strain rate effect. We can observe that the simulation results with the T-M model match fairly well with the experimental result of these complex buckling behaviors as a whole.

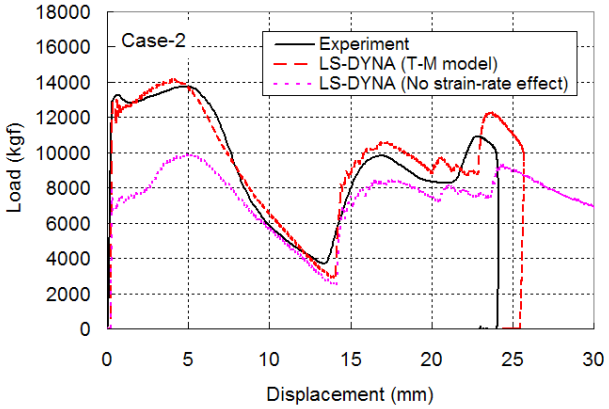

Fig. 14 Load-displacement curves of the hummer (Case-2)

Finally, the equivalent plastic strain contour at the bottom of the tube of Case-2 is shown in Fig. 15. The circular symbol indicates the observational point of the stress and the strain. We can observe that the maximum equivalent plastic strain is generated at the inner side of local buckling part of the tube, and the value is over largely the homogenous deformation region of the tensile test.

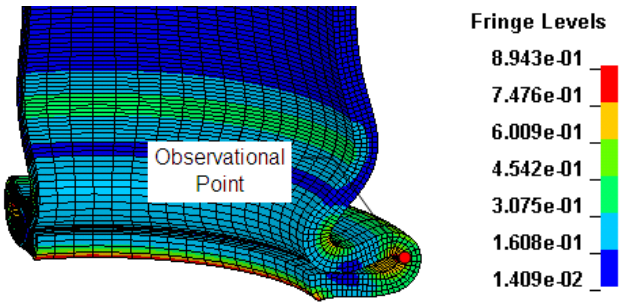

Fig.15 Equivalent plastic strain contour (Case-2)

The stress-strain curves at the observational point shown in Fig. 15 of Case-2 are shown in Fig. 16 (a). The broken curve indicates the simulation result using the T-M model. The dotted curve indicates the simulation result with no strain rate effect and is same to the quasi-static stress-strain curve shown in Fig. 11. Relationship between the equivalent plastic strain rate and the

equivalent plastic strain obtained by the simulation using the T-M model at the observational point shown in Fig. 15 is shown in Fig. 16 (b). We can observe that in Fig.16 (a) the stress-strain curve obtained using the T-M model becomes higher than that obtained with no strain-rate effect. It may be understood that the difference between two curves is caused by the strain rate effect corresponding to the strain rate histories shown in Fig. 16 (b).

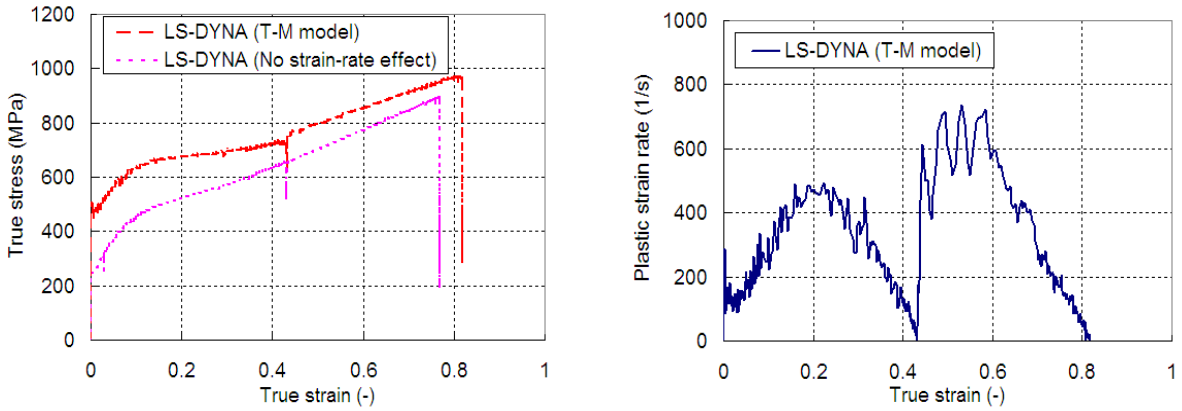

(a) Stress-strain curves (b) Plastic strain rate curve

Fig. 16 Simulation result of SS400 (Case-2)

Application in Crashworthiness

Tanimura-Mimura constitutive model was applied to full-lap front impact of a full vehicle onto a rigid wall as shown in Fig. 17. This original FEM model is 1977 Dodge Grand Caravan developed mainly for frontal impacts by the FHWA/NHTSA National Crash Analysis Center at the George Washington University [6]. The impact velocity is 56.2 kph. The model information is shown in Table 5. The total wall force in the simulation with the Tanimura-Mimura constitutive model (T-M model) is comparable with the NHTSA NCAP test result and with the simulation result with the Cowper-Symonds model (C-S model).

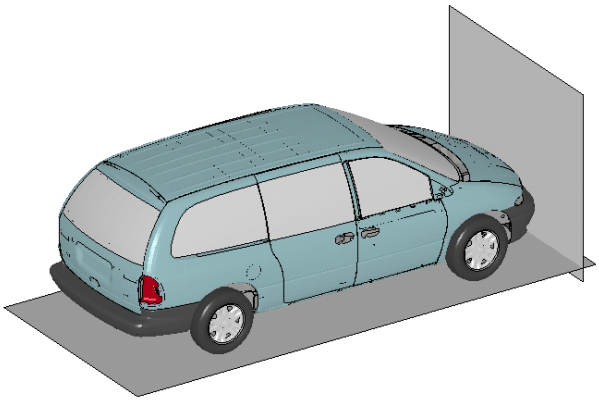

Fig. 17 Dodge Grand Caravan model

Table 5 FE model for Caravan

Number of Parts	510
Number of Nodes	344724
Number of Elements	333455
Solids	6253
Beams	35
Springs	4
Mass elements	317
Shells	327163

The deformation geometries after the impact were shown in Fig. 18. Figure 18 (a) shows the NCAP test results. Figure 18 (b) shows the simulation results with the T-M model. These two deformation geometries resemble each other approximately.

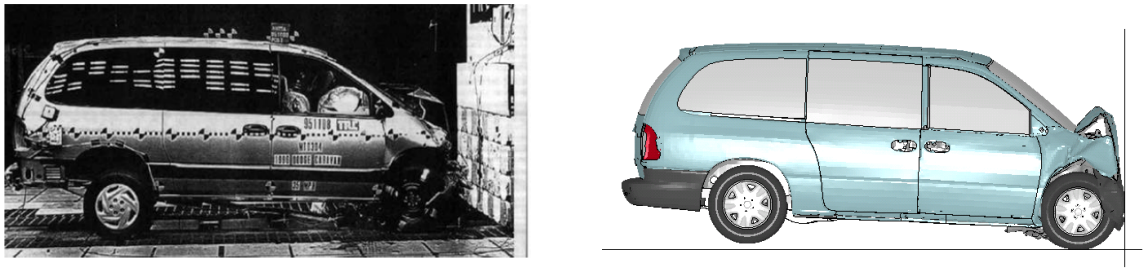

(a) Impact Test (b) LS-DYNA (T-M model)

Fig. 18 Full-lap front impact of Caravan

The wall force history curves were shown in Fig. 19. The solid curve indicates the experiment results, the dotted curve indicates the simulation results with the C-S model and the thick light green curve indicates the simulation results with the T-M model.

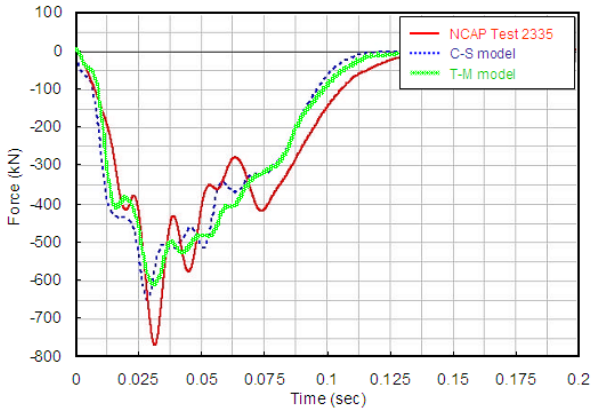

Fig. 19 Wall force

In this figure, the peak values of the simulation results of the C-S model and of the T-M model are about 15~20 % smaller than that of the experiment results. We stress that, while in the case of the C-S model, the values of the material parameters (e.g. C and P) of the material concerned are required in advance, in the case of the T-M model on the other hand, only the quasi-static stress-strain curve of the material concerned is required in advance. Considering these points, it is clear that, even for the simulation of the full-lap front impact of a full vehicle, the T-M model is useful not only for the high accuracy but also for using with little effort.

Conclusion

The Tanimura-Mimura constitutive model was implemented in LS-DYNA using defined user material model. We applied this Tanimura-Mimura model to several behaviors and showed that this model can be used very easily and effectively to simulate dynamic behavior in

crashworthiness studies and others over the wide strain rate range and over the entire range of strain reaching the fracture strain.

In the current version, the solid and shell elements are available for this model and the implemented material groups are only for the groups of ferrous materials and aluminum alloys. In a future version, the addition of the beam element and the resin material is scheduled.

References

[1] Tanimura, S., Mimura, K., and Zhu, W.H., Practical Constitutive Models Covering Wide Ranges of Strain Rates, Strains and Temperature, *Key Engineering Materials*, Vols. 177-180 (2000), pp. 189-200.

[2] Tanimura, S., Mimura, K., and Umeda, T., A Practical Constitutive Model Covering a Wide Range of Strain Rates for Various Grouped Metals, *J. Soc. Mat. Sci., Japan (in Japanese)*, Vol.50, N0.3, pp.210-216, Mar.2001.

[3] Tanimura, S., Hayashi, H., and Yamamoto, T., A practical constitutive model covering a wide range of strain rates and a large region of strain, *J. Phys. IV France*, Vol. 134 (2006), pp. 55-61.

[4] Tanimura, S., Hayashi, H., Yamamoto, T. and Mimura, K., Dynamic Tensile Properties of Steels and Aluminum Alloys for a Wide Range of Strain Rates and Strain, *Journal of Solid Mechanics and Materials Engineering*, Vol.3, No.12, 2009, pp.1263-1273.

[5] Tanimura, S., Uemura, M., Kojima, N. and Yamamoto, T., Recently Developed Testing Techniques and Dynamic Tensile Properties of Steels for Automobile, *Material Science & Technology 2004*, Conference Proceedings Volume I (AIST Proceedings), pp.481-490.

[6] http://crash.ncac.gwu.edu/pradeep/NCAP/caravan_ncap.pdf